



Zingiber officinale and thymus vulgaris extracts co-loaded polyvinyl alcohol and chitosan electrospun nanofibers for tackling infection and wound healing promotion

Hassan Maleki^{a,b,*}, Maryam Doostan^a, Kamyar Khoshnevisan^{c,d,e}, Hadi Baharifar^{e,f}, Saeid Abbasi Maleki^a, Mohmmad Amin Fatahi^g

^a Pharmaceutical Sciences Research Center, Health Institute, Kermanshah University of Medical Sciences, Kermanshah, Iran

^b Nano Drug Delivery Research Center, Health Technology Institute, Kermanshah University of Medical Sciences, Kermanshah, Iran

^c Medical Nanotechnology and Tissue Engineering Research Center, Shahid Beheshti University of Medical Sciences, Tehran, 1983963113, Iran

^d Department of Tissue Engineering and Applied Cell Sciences, School of Advanced Technologies in Medicine, Shahid Beheshti University of Medical Sciences, Tehran, Iran

^e Research and Development Team, Evolution Wound Dressing (EWD) Startup Co., Tehran, Iran

^f Department of Medical Nanotechnology, Applied Biophotonics Research Center, Science and Research Branch, Islamic Azad University, Tehran, 1477893855, Iran

^g Student Research Committee, Kermanshah University of Medical Sciences, Kermanshah, Iran

ARTICLE INFO

Keywords:

Nanofiber dressings
Infection
Wound healing

ABSTRACT

Infections are severe complications associated with chronic wounds and tardy healing that should be timely treated to achieve rapid and proper tissue repair. To hinder such difficulties, a nanofibrous mat composed of polyvinyl alcohol and chitosan (PVA/CS) was developed by electrospinning method, containing thyme (*Thymus vulgaris*) and ginger (*Zingiber officinale*) extracts. The mat containing 10 wt% of the extracts (at the ratio of 50:50) exposed the nanofibers (NFs) with the nanoscale diameter (average 382 ± 60 nm), smooth surface, and defect-free morphology. Likewise, the relevant analyses of the loaded mat displayed high wettability, porosity, and liquid absorption capacity without any adverse interaction. The obtained mat also provided a high antioxidant activity, and its release profile was continuous and sustained for nearly 72 h. Besides, it inhibited the growth of both Gram-positive *S. aureus* and Gram-negative *E. coli* strains. Furthermore, the proposed mat significantly accelerated cutaneous wound healing in bacterial-infected rats by preventing bacteria growth at the wound site. At last, histopathology analysis confirmed the ample regeneration of skin structures, forming collagen fibers and appendages. Overall, the proposed mat containing ginger-thyme extracts provides multiple therapeutic capabilities with promising solutions for inhibiting wound infection and accelerating the healing process.

1. Introduction

Mostly, after wounds are shaped, the skin system will commence the selected healing process containing hemostasis/inflammation

* Corresponding author. Address: Faculty of Pharmacy, Daneshgah Street, Kermanshah, Iran 6734667149.

E-mail address: Hasan.maleki@kums.ac.ir (H. Maleki).

<https://doi.org/10.1016/j.heliyon.2023.e23719>

Received 23 June 2023; Received in revised form 9 December 2023; Accepted 12 December 2023

Available online 16 December 2023

2405-8440/© 2023 The Authors. Published by Elsevier Ltd. This is an open access article under the CC BY-NC-ND license (<http://creativecommons.org/licenses/by-nc-nd/4.0/>).

Table 1Most compounds present in the *Thymus* and ginger extract were analyzed by GC–MS to represent the benefits for the skin.

<i>Thymus</i> extract	No.	Compound	Molecular formula	Retention time (min)	Percentage (%)	Advantages/wound healing activity
	1	α -Pinene	C ₁₀ H ₁₆	6.546	0.18	Antioxidant, anti-inflammatory, chondroprotective
	2	Camphene	C ₁₀ H ₁₆	6.998	0.13	Hypolipidemic, hepatoprotective
	3	β -Myrcene	C ₁₀ H ₁₆	8.491	0.15	Antioxidant, antiulcer, anticancer
	4	Carene	C ₁₀ H ₁₆	9.389	0.27	Antioxidant, anti-inflammatory
	5	<i>p</i> -Cymene	C ₁₀ H ₁₄	9.704	2.77	Antioxidant, antimicrobial
	6	γ -Terpinene	C ₁₀ H ₁₆	11.060	1.18	Antimicrobial, antioxidant
	7	α -Terpineol	C ₁₀ H ₁₈ O	16.811	0.28	Antimicrobial
	8	Thymol	C ₁₀ H ₁₄ O	21.354	3.82	Antimicrobial, antioxidant
Ginger extract	1	Isoleucine	C ₆ H ₁₃ NO ₂	0.50	131.0947	Promotion of the skin's natural ability to regenerate
	2	Phenylalanine	C ₉ H ₁₁ NO ₂	0.69	165.0785	Retaining moisture for a more hydrated appearance
	3	(<i>Z</i>)-citral	C ₁₀ H ₁₆ O	2.66	152.1197	Antimicrobial, antifungal, and antiparasitic
	4	Galanganol C	C ₂₇ H ₂₈ O ₅	4.07	432.1937	Soothing eczema, burn and itchiness, and fungal infections
	5	Zingerone *	C ₁₁ H ₁₄ O ₃	6.71	194.0942	Help with visible repair, and nurtures skin's ability to maintain the integrity of the extracellular matrix
	6	Dihydrocurcumin	C ₂₁ H ₂₂ O ₆	7.75	370.1402	Decreasing inflammation and oxidation
	7	Tetrahydrocurcumin	C ₂₁ H ₂₄ O ₆	11.58	372.1557	Antioxidant activity and depigmentation of the skin
	8	(<i>E</i>)-7-(3,4-dihydroxyphenyl)-1-(4-hydroxy-3-methoxyphenyl)hept-2-en-1-one	C ₂₀ H ₂₂ O ₅	12.00	342.1451	antineoplastic

phase, proliferation phase, and remodeling phase [1,2]. The physiological wound healing process can be provided via the improvement and maintenance of a moist and neat wound area. In addition, the prevention of wound infections is the first target in common wound control. In this case, the priority is to obtain a decline in microorganism quantity on the wound surface using the common practical methods including debridement, therapeutic cleansing, applied antimicrobial agents, and so on.

Bacteria-caused infections are in charge of over millions of death, so that skin and tissue infections are extensively predictable kinds of infections that annually touching more than 10 million people in the United States [3]. In order to speed up the healing process of an infected wound, many strategies have been developed. Among these, wound dressings have been taking more attention for many diverse uses due to effectiveness, and accessibility [4].

Regarding wound and patient status, a proper wound dressing must be opted in. Medicated wound dressings are obtained from both, natural and synthetic materials loaded with a therapeutic agent, in different physical types such as ointments, hydrogels, fibers, or nanofibers (NFs) [5]. In recent years, electrospun NFs have been extensively applied as the foundation of wound dressings for wound healing promotion [4]. Electrospinning is an accessible, effective, and commercial technique, using a high-voltage field to produce NFs [6,7]. NFs also can be loaded with therapeutic agents, and then after that applied for the acceleration of wound healing [8,9].

Natural compounds loaded into synthetic and natural polymer mixtures were extensively employed for wound healing promotion by stimulating one of the healing phases over anti-inflammatory, antimicrobial, and antioxidant attributes. Poly (vinyl alcohol) (PVA) is generally applied as a biopolymer for NF generation owing to safe, high water solubility, biodegradability, and biocompatibility [10, 11]. Besides, NFs made of PVA polymer displayed remarkable mechanical properties and chemical resistance with a high swelling ability [12,13]. In the case of cost-effective and practical natural polymer, chitosan (CS) is a heteropolysaccharide containing glucosamine and *N*-acetyl glucosamine units linked to $\beta(1-4)$ glycosidic bonds [14]. CS provides various intrinsic properties including adhesive capability, antimicrobial, and antifungal activity, and also renders biocompatibility, and biodegradability [15,16].

Ginger (*Zingiber officinale Roscoe*), one of the monocotyledons types, is the rhizome of the Zingiberaceae plant family [17]. Ginger has been considered and investigated for various ranges of biological assessments such as analgesic, antitumor, antifungal, antioxidant, anti-allergic, anti-inflammatory, and antimicrobial thanks to its notable medical and biological properties [18]. Ginger extracts have been applied in hydrogels, and composites as antimicrobial, antifouling, and antioxidant agents for food packaging applications [19–21]. However, it is seldom considered to be a nanofibre or involved in a nanofibre owing to its complex components.

Thyme (*Thymus vulgaris*), one of the family Lamiaceae, has been considered for antifungal and antioxidant activity owing to phytochemicals' ability in the extract [22,23]. Thyme provides a prospective basis of fruitful bioactive agents with several pharmacological features, comprising antioxidant, antimicrobial, and anti-inflammatory capability, causing thyme a favorable candidate in wound healing process [24,25].

Wound healing promotion by using electrospun NFs containing thyme and ginger as natural agents has been studied in a few cases. For instance, in one study, the cost-effective fabrication of ZnO NPs beginning from proper precursor and ginger was investigated. The proposed electrospun NFs were successfully prepared by a green precipitation approach and also can be applied for wound dressing application [26]. In another study, electrospun PVA NFs in combination with hydroalcoholic solutions of thyme, *Salvia officinalis folium*, and *Hyperici herba* as phytotherapeutic agents were applied for wound healing application. The proposed NFs displayed an admitted antibacterial activity [27].

To the best of our knowledge, no study has been considered to develop electrospun NFs along with both thyme and ginger with remarkable ability in biological activity for wound healing application. Table 1 Has been provided to exhibit the most common compounds present in the thyme and ginger extract, retention time, the percentage (%), and advantages of each component, based on literature review and data investigation [28,29].

In this study, a polyherbal (extracts)-loaded electrospun NFs composed of PVA and CS polymers was proposed for wound healing promotion. The most common characterization of the obtained wound dressing has been carried out to confirm the fabrication process as well as the biological ability such as histological and antibacterial assessments. Finally, the proposed wound dressing was carried out for the study of *in vitro* and *in vivo* antibacterial and wound healing process.

2. Materials and methods

2.1. Materials

Poly (vinyl alcohol) (PVA, Mw: 72,000 Da), chitosan (CS, Mw: 190,000–300,000 Da, 75–85 % deacetylated), phosphate buffer saline (PBS), and 2,2a-Diphenyl-1-picrylhydrazyl (DPPH) were purchased from Sigma Aldrich (United States). Nutrient broth and nutrient agar were provided from Gibco Co. (The Netherlands), and ketamine and xylazine were supplied from Alfasan Co. (the Netherlands). All used solvents in the experiments were of analytical grade and obtained from Dr Mojalali Co., Iran. Bacterial strains, *E. coli* (ATCC 2592) and *S. aureus* (ATCC 25923), were procured from the Pasteur Institute of Tehran, Iran.

2.2. Preparation of extracts

First, the identification of plant species, i.e., *Thymus vulgaris* (thyme) and rhizomes of ginger (*Zingiber officinale Rosc.*), was conducted through macroscopic methods by a botanical expert, supported by pharmacognosy reference books and online databases. Then, as previously reported to obtain hydroalcoholic extracts by maceration method [30,31], the fresh aerial parts of *Thymus vulgaris* and rhizomes of ginger (*Zingiber officinale Rosc.*) were separately shade-dried at room temperature and pulverized. Afterwards, they were immersed in 70 % ethanol for 72 h in a shaker at 25 °C. Then, the mixtures were filtered through filter paper (Whatman No. 42) and

dehydrated in a rotary evaporator at 45 °C for 24 h. Lastly, the obtained extracts were collected and stored at 4 °C for subsequent use.

2.3. Fabrication of extracts co-loaded electrospun NFs

The electrospinning technique was applied to prepare blank PVA/CS NFs [32]. First, 10 % w/v of PVA dispersion in distilled water and 2 % w/v of CS dispersion were prepared in acid acetic 1 %. Next, the prepared mixture at the ratio of 80:20 v/v PVA:CS dispersions was mixed properly and subjected to electrospinning process by imposing 20 kV applied voltage, 15 cm needle-tip-to collector distance, feeding rate 1 mL/h at room temperature (25 °C). Then, the proposed NFs were examined in terms of morphology and diameter distribution. After that, 10 wt% of *Zingiber officinale* and *Thymus vulgaris* extracts (Ginger: Thyme 100:0, 0:100, and 50:50 % w/w) were added to the PVA/CS solution and mixed well (Table 2). The blended solutions were electrospun in the same setting to fabricate the fibrous mats with the proper thickness on an aluminum rotating drum. Finally, the obtained mats were removed from the drum, cross-linked with glutaraldehyde vapor and preserved for further characterizations.

2.4. Diameter and morphology characterization

The morphology and diameter of the prepared mats were determined by SEM (HITACHI S-4700, Japan) at an accelerating voltage of 25.0 kV. All samples were cut into 1.5 × 1.5 cm pieces and coated with gold, then their diameter and distribution were evaluated using Image J software.

2.5. Infrared spectroscopy analysis

The chemical groups and interactions of the materials in the samples, including free extracts, free NF, and extracts-loaded NFs, have been investigated using the FTIR spectrophotometer (Shimadzu, IR Affinity-1, Japan) at 20 °C from 400 to 4000 cm⁻¹.

2.6. Porosity, wettability, and water absorption capability

The porosity of the obtained mats was evaluated by the liquid displacement method [32]. Desired pieces of each mat were immersed in a specific weight of ethanol. After 1 h, the weight of the ethanol, having the dipped pieces, was measured. Then the mat was removed, and the weight of the ethanol was retaken. Finally, the porosity percentage of NFs was obtained using equation (1).

$$\text{Porosity \%} = \left(\frac{V1 - V3}{V2 - V3} \right) \times 100 \quad [1]$$

V1 is the ethanol's initial weight, V2 is the weight of ethanol plus immersed NF, and V3 is the weight of ethanol after NF removal.

The sessile drop technique was used to evaluate the contact angle (CA), which determines the wettability of the fibers' surface. Briefly, 4 μL of distilled water were placed on the surface of the samples, and their images were recorded immediately at room temperature. All measurements were performed in triplicate, and average values were reported.

To estimate the swelling rate of the prepared NFs, they were cut into 1.5 × 1.5 cm pieces and weighed. Then each sample was placed in the PBS at 37 °C. After specific time intervals (i.e., 1, 3, 6, 12, 24 h), the samples were removed from the buffer, and a filter paper was used to dry their surface water gently. Then the fiber pieces weight was measured, and the swelling rate was calculated using equation (2):

$$\text{welling \%} = \frac{W_{\text{wet}} - W_{\text{dry}}}{W_{\text{dry}}} \times 100 \quad [2]$$

Wwet: wet weight and Wdry: dry weight.

2.7. Free radical scavenging assay

The antioxidant activity of the prepared NFs was carried out by DPPH radical scavenging assay [33,34]. First, equal concentrations of the samples were added to 3 mL of 10⁻⁴ M DPPH methanolic solution. Then the solution was incubated in the dark for 30 min at room temperature. Finally, the solution absorbance (A_{sample}) was read out at 517 nm against the blank (A_{control}) using a UV-Vis spectrophotometer (Cecil Instruments Ltd., UK), and the percentage of antioxidant activity was calculated by equation (3).

Table 2

The composition of fabricated electrospun nanofibers.

Nanofiber type	Composition
Blank (free) PVA/CS NFs	PVA:CS (80:20 v/v)
Thyme-loaded NFs	PVA:CS (80:20 v/v) loaded with 10 wt% of <i>Thymus vulgaris</i> extract
Ginger-loaded NFs	PVA:CS (80:20 v/v) loaded with 10 wt% of <i>Zingiber officinale</i> extract
Ginger:thyme loaded NFs.	PVA:CS (80:20 v/v) loaded with <i>Zingiber officinale</i> extract (5 wt%) and <i>Thymus vulgaris</i> extract (5 wt%)

$$\text{Antioxidant activity (\%)} = \left[\frac{(A_{\text{control}} - A_{\text{sample}})}{A_{\text{control}}} \right] \times 100 \quad [3]$$

2.8. In vitro release assessment

The calibration curve of ginger extract and thyme extract were obtained using the extract solutions (in the 0–100 µg/mL range) including 0.1 M PBS medium (pH 7.4). Absorbance values were measured at the wavelengths of 276 nm (λ_{max} for ginger extract) [35] and 330 nm (λ_{max} for thyme extract) [36] using a quartz cuvette. In the following, 25 mg of the ginger-thyme loaded NFs immersed in 50 mL of PBS containing Tween 80 (2 % w/v) (pH 7.4) were placed in a shaker incubator at 37 °C under 250 rpm constant agitation. At specific time intervals (1, 2, 3, 6, 12, 24, 48, and 72 h), 2 mL of the medium was withdrawn and replaced with fresh PBS. The concentration of the loaded extracts in the removed sample was measured by UV-vis spectrophotometer from the related standard curve (absorbance vs. concentration). The cumulative release was calculated at that particular time, and the release profile of the extracts from the obtained mats was determined.

2.9. In vitro antibacterial activity determination

The bacterial growth inhibition potential of the NF samples was assessed using the agar-disk-diffusion method on *S. aureus* (ATCC 25923) and *E. coli* (ATCC 25922) bacteria commonly found in skin infections, following the guidelines of the Clinical and Laboratory Standards Institute (CLSI) [37]. Briefly, a bacterial suspension was prepared at a 0.5 McFarland standard (1.5×10^8 Colony Forming Units per mL, CFU/mL) and inoculated onto nutrient agar plates. For inoculation using a sterile cotton swab, the bacteria were evenly spread across the entire plate's surface by swabbing in three different directions. Circular discs (1 cm in diameter) were cut from the NFs and sterilized by 3 h of UV exposure on each side. These discs were then placed on the bacteria-inoculated plates and incubated for 24 h at 37 °C. Finally, the inhibition zone diameters of each sample were measured around the closest colony to the disk and photographed.

2.10. In vivo wound healing assessment

2.10.1. Infected wound induction, grouping and treatments

The animal studies were performed under the Ethic Committee for Animal Experiments of Kermanshah University of Medical Sciences (IR.KUMS.AEC.1401.005). The animal studies were performed under the EU Directive 2010/63/EU for animal experiments and subsequent amendments or comparable ethical standards. Male, 8–10 week old Wistar rats with mean weight 220 ± 20 g were used for induction of infected wounds. Rats were fed *ad libitum* and kept under specific pathogen-free conditions. Before each skin wound formation, the animals were intraperitoneally anesthetized with a mixture of Ketamine: Xylazine (80:10 mL/kg). Then a round section of skin injury (2 cm in diameter) was made on the back of each rat using a sterile biopsy apparatus. After that, the infection model was engendered with inoculation of wounds with 25 µL of *S. aureus* suspension (ATCC 25923, 10^7 CFU in PBS) and kept uncovered for 15 min to allow the bacterial dispersion to penetrate in the wounded skin [38]. Subsequently, on 1, 7, and 14 days, a sterile cotton swab was applied to gently eliminate the wound sites. They were spread cultured on agar plates and then incubated for 24 h at 37 °C to evaluate the anti-infection activity.

Thirty-five wound-infected rats were randomly divided into 7 groups (N = 5) and every three days were treated with the following administration.

- i) negative control (without treatment only covered with sterilized gauze); ii) treated with thyme extract; iii) treated with ginger extract; iv) treated with blank PVA/CS NFs; v) treated with thyme extract-PVA/CS NFs; vi) treated with ginger extract- PVA/CS NFs and vii) treated with thyme-ginger extracts- PVA/CS NFs.

2.10.2. Wound healing assessment

Macroscopic wound healing was measured with the determination of wound area and wound closure. In this regard, the wound sites were photographed on days 0 (after wound creation), 1, 5, 9, 10, and 14. The wound area was measured with Image J software and the average values were reported. In addition, the rate of wound closure was measured by tracing the wound area in the specified days by the following formula (Equation (4)):

$$\text{Wound closure \%} = \left[\frac{W_{t_0} - W_{t_i}}{W_{t_0}} \right] \times 100 \quad [4]$$

Where W_{t_0} was the wound area on day 0 and W_{t_i} was the wound area on the day of examination.

2.10.3. Histopathological analyses

On the 14th day, the healed wound sites with full thickness were isolated and fixed in 10 % formaldehyde solution. Then, the wound samples were embedded in paraffin, cut into 5-mm thick sections and stained with hematoxylin and eosin (H&E) and Masson's trichrome. The stained sections were photo-captured by an optical microscope and tissue regeneration was analyzed based on histopathological evaluation.

2.11. Statistical analysis

All experiments were performed in triplicate, and the mean \pm SD was reported. Image J software was applied to calculate the diameter distribution of NFs. All data and graphs were analyzed using Graph Pad Prism 9, and OriginPro 2020. The significance level of the difference between the groups was considered as a p-value $<$ 0.05.

3. Results and discussion

One of the most severe issues in wound management is bacterial infections, which can significantly impair and delay the wound healing process [39]. Hard-to-heal and chronic wounds are predisposed to the colonization and proliferation of microorganisms. Thus, applying wound dressings releasing anti-bacterial agents is indispensable for the prevention or even elimination of potential bacterial infections. Electrospun NFs as novel materials can provide multifarious properties, capable of loading natural substances to fulfill the requirements for an efficient anti-infection wound dressing. Therefore, PVA/CS NFs were first made by electrospinning method, then loaded with two prepared extracts and the diameter distribution and morphology of NFs were microscopically investigated.

3.1. Diameter and morphological characterization

Electrospinning of 80:20 v/v PVA: CS mixture resulted in the homogeneous production of fibers with a smooth surface and a diameter distribution of 210 ± 30 nm and without any bead (Fig. 1A). Incorporation of 10 wt% ginger extract led to the formation of NFs having a uniform morphology with an average diameter of 295 ± 62 nm (Fig. 1B). In addition, the SEM micrograph indicated loading 10 wt% thyme extract produced the NFs having a uniform shape with the diameter distribution of 307 ± 94 nm (Fig. 1C). After adding 10 wt% ginger-thyme extracts (50:50) in PVA/CS solution, the diameter of prepared fibers was increased to an average 382 ± 60 nm (Fig. 1D). This increase was possibly attributed to the increasing viscosity of the polymeric mixture and physical intermolecular interaction between polymer chains and the extracts [40,41]. The inclusion of the higher amount of extracts ($>$ 10 wt%) led to the production of non-homogenous fibers in shape and diameter containing the structural defects e.g., beads and drops, which could reduce the active surface area of NFs and affect the release profile [42]. As a result, the NFs containing 10 wt% of the extracts were selected for further experiments.

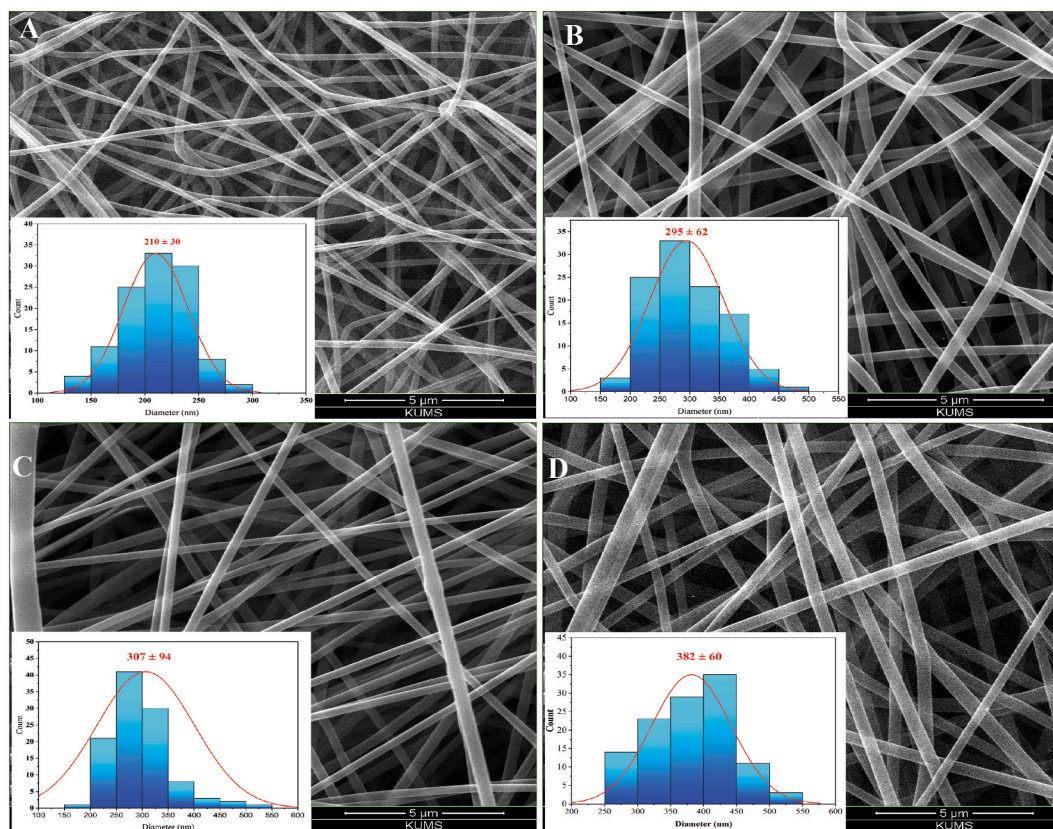


Fig. 1. SEM micrograph of electrospun PVA/CS NFs (A), and the NFs incorporated with 10 wt% ginger extract (B), 10 wt% thyme extract (C) and 10 wt% ginger-thyme (50:50) extracts (D) with the corresponding size distribution histograms.

3.2. FTIR characterization

To investigate the functional groups and the interaction between the constituents of NFs and to confirm the presence of extracts in the resultant NFs, FTIR spectroscopy was performed and the obtained spectra were depicted in Fig. 2. The spectrum of free PVA/CS NFs exhibits distinctive sharp peaks at 1093 cm^{-1} and 1250 cm^{-1} attributed related to C–O stretching of ether groups and the intense peak at 1734 cm^{-1} related to C=O stretching of PVA and acetyl groups in CS polymer [43]. The absorption peaks at 2920 cm^{-1} and 2935 cm^{-1} are attributed to the stretching vibration of the $-\text{CH}_2$ group. Also, a wide absorption band appearing at $3200\text{--}3500\text{ cm}^{-1}$ is corresponding to the $-\text{OH}$ stretching of the inter and intra molecular hydrogen in PVA and CS overlapped with the $-\text{NH}_2$ vibration of the primary amines of CS [44]. The spectrum of thyme extract (*Thymus vulgaris*) observed in the peaks of 1045 cm^{-1} , 1641 cm^{-1} , 2924 cm^{-1} and 3414 cm^{-1} , which is respectively related to C–O, C=O, N–H stretching bonds and $-\text{OH}$ group; these peaks are related to the main phenolic compounds of the extract such as thymol and carvacrol [45,46]. In addition, the spectrum of ginger extract (*Z. officinale*) shows characteristic peaks around 1091 cm^{-1} , 1249 cm^{-1} , 1730 cm^{-1} , 2910 m^{-1} , and 3280 cm^{-1} wavenumbers that correspond to C–O, C–N, C=O, N–H stretch and broad peak at $3200\text{--}3500$ related to hydroxyl groups, respectively; these peaks are related to the flavonoid, phenolic and terpenic compounds in the extract [47,48]. In the spectra of thyme-PVA/CS NFs and ginger-PVA/CS NFs, there are characteristic peaks related to thyme extract and ginger extract, which indicate the loading of the extracts, just slightly, the intensity or position of C=O stretching were altered possibly due to physical interaction with the polymeric matrix of the NFs. For ginger: thyme-PVA/CS NFs, the obtained spectrum confirms the presence of both extracts in the NF structure owing to the main distinct peaks of ginger and thyme extracts appeared in the fabricated NFs as well as the characteristic peaks of PVA and CS polymers are clearly defined. However, some peaks were slightly shifted to lower or higher wave numbers and/or overlapped due to physical intermolecular interactions.

3.3. Porosity, wettability, and water absorption capability results

Porosity plays a key role in the function of wound dressings. The porosity measurement revealed that free PVA/CS NFs, ginger-loaded NFs, thyme-loaded NFs, and ginger: thyme-loaded NFs displayed 89.2 %, 92.7 %, 93.1 %, and 92.6 % porosity of the total volume, respectively (Fig. 3A). The loading of the extract(s) raised the value of porosity, however the percentage was not remarkable ($p > 0.05$). It was probably due to the increase in the pore size of the mats that is evident in the microscopic images. These findings indicate the nanofibrous mat's abundant porosity that could provide high permeability for nutrients and gases and absorption of exudates [49,50].

The CA of the prepared mats was assessed as an indicator of wettability and hydrophilicity, which in turn can influence the absorption of fluids, maintaining the moisture in wound sites, cell adhesion, and proliferation [33,51]. The average CA value for the free PVA/CS NFs, ginger-loaded NFs, thyme-loaded NFs and ginger: thyme-loaded NFs were about 17.4° , 24.2° , 25.5° and 25.5° , respectively (Fig. 3B). Furthermore, all mats' CAs terminated to 0° after 10 s, and the extract(s) loading did not significantly switch on CA value. The results indicated the mat surface with very high wettability and hydrophilicity.

The water absorption capability of the prepared NFs is shown in Fig. 3C. In 30 min of immersion, the average percentage of water absorption for free PVA/CS NFs and ginger:thyme-loaded NFs was $223 \pm 15\%$ and $288 \pm 22\%$, and also after 24 h immersion reached about $607 \pm 15\%$ and $674 \pm 11\%$, respectively. After loading the extracts, water absorption capability improved, and the obtained value indicates that it can absorb the excessive exudate and maintain a moist environment [44,51].

3.4. Antioxidant activity

The free-radical scavenging activities of the prepared NFs are displayed in Fig. 4. At concentrations $25\text{--}400\text{ }\mu\text{g/mL}$, the range of scavenging activities of free PVA/CS NFs, thyme-loaded NFs, ginger-loaded NFs and ginger:thyme-loaded NFs obtained about 2.5–6.8

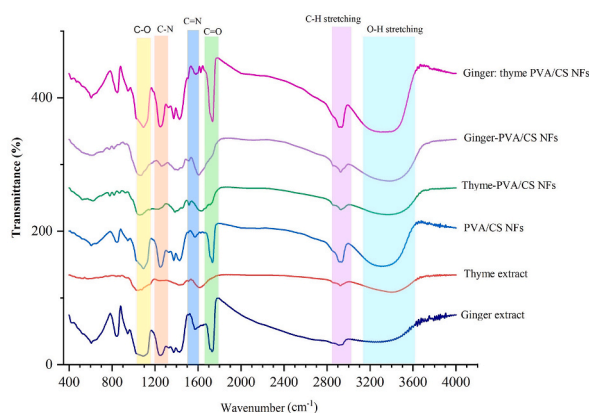


Fig. 2. FTIR spectra of free extracts, blank fabricated NFs, the NFs loaded with the extracts separately and concurrently.

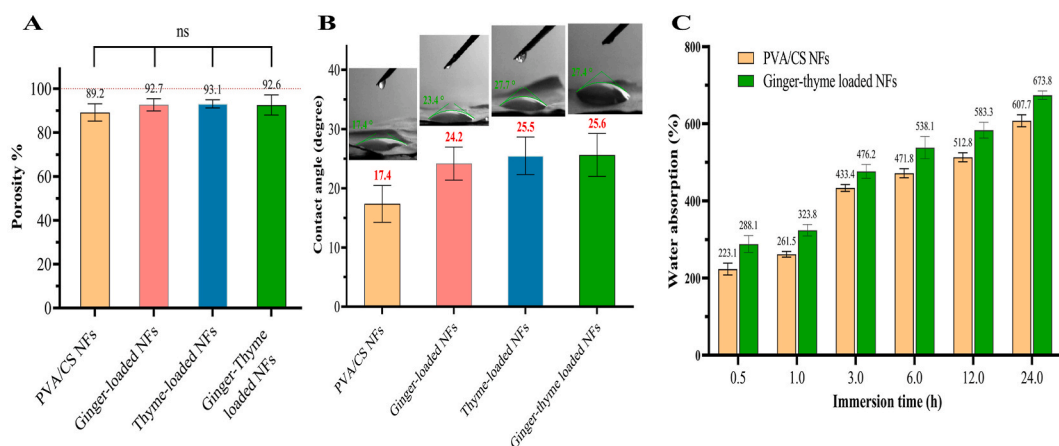


Fig. 3. Porosity values (A), water contact angle (B) and water absorption capacity (C) of the prepared NFs. (Average values are presented above the columns; ns indicates $p > 0.05$).

%, 4.8–56.8 %, 13–73.5 % and 19.8–96.5 %, respectively. The blank PVA/CS NFs did not show considerable antioxidant activity. While the NFs containing thyme and ginger separately demonstrated that they could scavenge free-radical oxidants, which proved the antioxidant capability of the active components present in the extracts. Besides, the highest percentage of DPPH scavenging potential was observed by ginger: thyme-loaded NFs at the same concentrations. The findings indicate the combined antioxidant effect of the compounds in the extract and, therefore, conferring remarkable protection against oxidative stress-mediated injuries to promote wound healing process [52,53].

3.5. *In vitro* release study

Fig. 5 displays the *in vitro* release profile of the extracts from ginger: thyme (50:50)-loaded nanofibrous mats in 3 days (72 h). As observed, the extracts' release profile was time-dependent, and after 6 h, 28.3 ± 4.3 % and 45 ± 4.2 % of thyme and ginger extracts released, respectively., the amount released of thyme and ginger extracts reached 63.7 ± 4 % and 80 ± 5.7 %, respectively within 24 h. After the release time of 72 h, 87.5 ± 3.5 % and 95.5 ± 3.5 % of thyme and ginger extracts released from ginger: thyme NFs, respectively. Therefore, the extracts release profile from the NFs indicated that the extracts sustainably released from the polymer matrix for 72 h. The release of thyme extract had advanced with a lower diffusion rate out of the matrix, probably due to the more hydrophobic compounds in the extract, e.g., thymol and carvacrol. The prepared NFs with continuous and sustained release of the

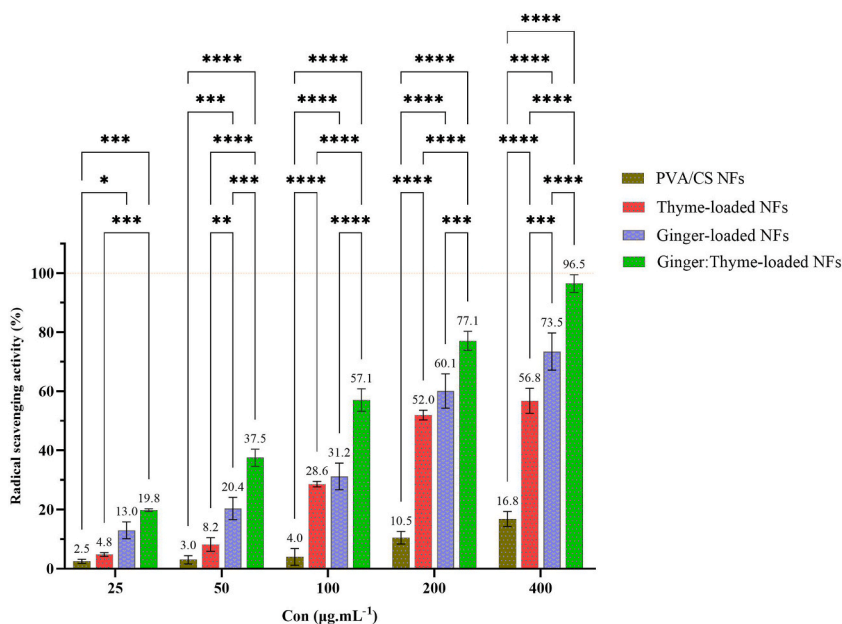


Fig. 4. DPPH scavenging activity of the prepared nanofibrous mats. (** indicates $p < 0.01$, *** $p < 0.001$, **** $p < 0.0001$).

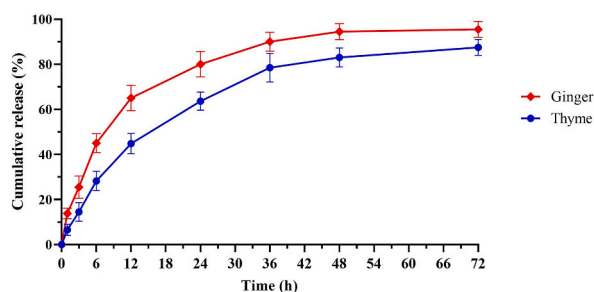


Fig. 5. The *in vitro* release profile of the extracts from ginger:thyme (50:50)-loaded nanofibrous mats in phosphate buffer (pH 7.4).

loaded compounds can provide long-term effects and reduce the consumption of large doses of drugs necessary to inhibit and destroy microorganisms effectively [54,55].

3.6. *In vitro* antibacterial activity

Antibacterial activity of the prepared NFs against Gram-positive (*S. aureus*) and Gram-negative (*E. coli*) bacteria was assessed by agar disk diffusion method. As depicted in Fig. 6, the free PVA/CS NFs did not exhibit either inhibition of bacterial growth or killing on both strains, therefore no inhibition zone was observed around it. Ginger-loaded NFs proposed only little broad inhibition zones with an average diameter of 12 ± 2 mm on both bacterial strains. On the other hand, thyme-loaded NFs indicated broad inhibition rings 15 ± 4 mm in diameter, which might be due to the release of potent antimicrobial substances in the extract [56]. Besides, ginger: thyme-loaded NFs have shown great antibacterial inhibition by creating zones with a diameter of 18 ± 3 mm. The presence and combination of the components of both extracts resulted in enhancing the antibacterial potential of these nanofibrous mats [57,58].

3.7. Wound healing efficacy

To evaluate the healing of the wounds, imaging was performed from the wound sites in the various treatment groups, as shown in Fig. 7. In the negative control group, a slow progression was observed in wound healing process over 14 days (Fig. 7A). As comparative treatments, the free extracts were also applied distinctly, so treatment with thyme and ginger extracts accelerated wound healing compared to the negative control (Fig. 7B and C). The group treated with free PVA/CS NFs improved wound repair and caused faster wound healing compared to the negative control (Fig. 7D). While the groups treated with the NFs containing thyme and ginger extracts separately accelerated wound healing better and more than their free form, as well as on day 14, a significant part of the wound healed (Fig. 7E and F). In the treated group (NFs containing ginger: thyme extracts), the best wound healing process was achieved, and on days 5, 9, and 14, great wound healing was obtained compared to other groups (Fig. 7G). Besides, after 14 days, the wound area was completely repaired and the least area of the wound and scar remained. Furthermore, the quantitative size of the wound area in different treatment groups was measured during the 14 days (Fig. 8A). The average wound area on the 14th day was 0.5 ± 0.05 cm², 0.44 ± 0.04 cm², 0.33 ± 0.06 cm², 0.49 ± 0.02 cm², 0.27 ± 0.02 cm², 0.19 ± 0.04 cm² and 0.05 ± 0.01 cm² for the negative control group, thyme extract, ginger extract, free PVA/CS NFs, the thyme-loaded PVA/CS NFs, the ginger-loaded PVA/CS NFs and ginger: thyme-loaded NFs, respectively. In the case of wound area, the comparison of the wound healing monitoring (day 14) between different groups is shown in Fig. 8B. Obviously, the lowest wound area was achieved in the group treated with NFs containing ginger: thyme extracts that were significantly lower than that of the other groups. In addition, the rate of changes of wound closure in different groups (Fig. 8C and D), indicated that the ginger:thyme-loaded NFs treated group provided nearly complete wound closure (above 98

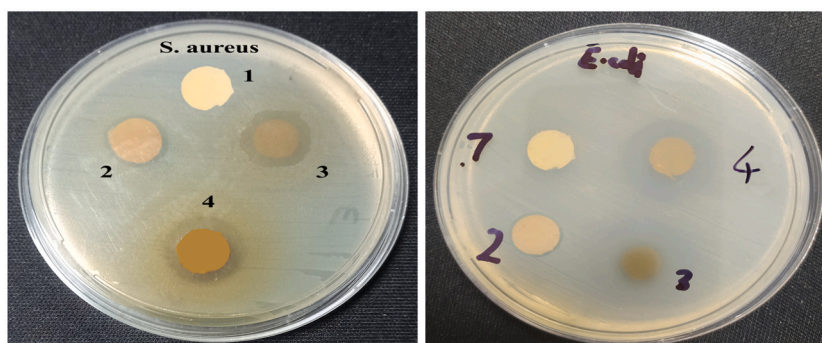


Fig. 6. Antibacterial activity against *S. aureus* and *E. coli* bacteria, the numbers 1, 2, 3, and 4 represent free PVA/CS NFs, ginger-loaded NFs, thyme-loaded NFs, and ginger:thyme-loaded NFs, respectively.



Fig. 7. Alteration trend of the morphology of the infected wounds treated with different samples over 14 days; negative control (A), thyme extract (B), ginger extract (C), free PVA/CS NFs (D), NFs containing thyme extract (E), NFs containing ginger extract (F), and NFs containing ginger:thyme extracts (G).

%) within 14 days with a significant difference from the other treatments. Whereas in the other groups, wound closure was incomplete and extremely scar tissue remained at the wound sites. It seems that owing to synergic effect of the natural compounds, the obtained mat with both thyme and ginger extract rendered a promising solution to hard-to-close wound treatment.

3.8. *In vivo* anti-infective efficacy

Wound infection generated by pathogenic microorganisms delays wound healing and causes lethal bacteria in severe circumstances. Therefore, inhibiting bacteria growth in wound sites is imperative to preventing wound infections and accelerating tissue regeneration [59]. Hence, after sampling from the wound sites, the growth of bacteria in the agar culture medium was determined and photographed. As can be seen in Fig. 9A, on the first day, the bacteria grew entirely, and the wound environment was full of bacteria in all groups. On day 7, the negative control group and the groups treated with thyme extract (Fig. 9B), ginger extract (Fig. 9C), and free PVA/CS NFs (Fig. 9D) did not show a significant difference in the inhibition of bacterial growth. Although the number of bacterial colonies decreased in the groups treated with NFs containing thyme extract and ginger extract (Fig. 9E and F), it did not entirely inhibit bacterial growth. In contrast, the growth of bacteria in ginger:thyme-loaded NFs significantly decreased, indicating the proficient effect of inhibiting infection at the wound site (Fig. 9G). On day 14, remarkable bacterial growth appeared in the wound site of the control negative, thyme extract, ginger extract, and free PVA-CS NFs groups and exhibited no complete antibacterial activity. Compared to the previous groups, the groups treated with NFs containing thyme extract and ginger extract led to a greater decrease in the bacterial count, though the total eradication of infection after treatment was not achieved. As if in ginger:thyme-loaded NFs, no bacterial colonies developed in the culture medium, so the bacteria's growth was completely inhibited, which proved its high potency anti-infective efficacy to achieve hasty wound healing.

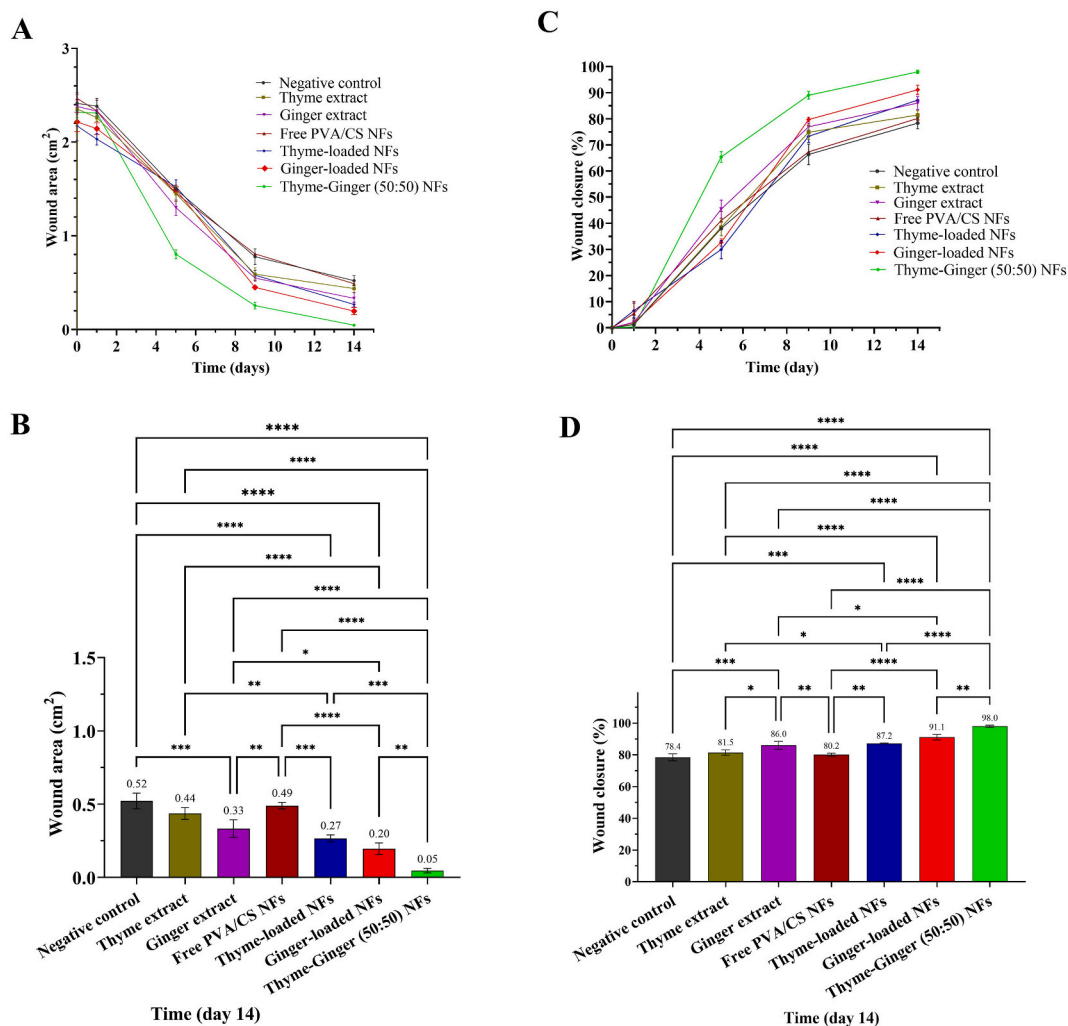


Fig. 8. Analyzing the changes in wound area during the 14-day wound healing period (A) and at the end of the 14th day (B), and the changes in wound closure during the 14-day wound healing period (C) and at the end of the 14th day (D). (Mean values are presented above the columns; * indicates $p < 0.05$, ** $p < 0.01$, *** $p < 0.001$, and **** $p < 0.0001$).

3.9. Histopathological examination

H&E staining was applied to clearly study the regeneration of the skin structure and the related layers under bacterial infection on day 14, and results are displayed in Fig. 10. Control animals show an incomplete skin structure with separated dermis the epidermis along with microvascular bleeding (Fig. 10A). The treated wound with free thyme and ginger extracts indicated that the thin and incomplete epidermis was formed as a regular epithelium, the dermis immaturely integrated into the epidermal layer, and new immature blood vessels are evident (Fig. 10B and C). In the group treated with PVA/CS NFs, the dermis and epidermis layers were regenerated immaturely, and slightly new and immature blood vessels and skin appendages were also visualized in the dermis (Fig. 10D). Moreover, in the groups treated with NFs containing thyme extract and ginger extract, the skin tissue still had progression at the regeneration and maturation, the epidermis and dermis layers integrated, and the numerous new blood vessels were appeared (Fig. 10E and F). In particular, the ginger:thyme-loaded NFs exhibited the formation of a new entire regenerated epidermis that confers intact re-epithelialization and wound closure (Fig. 10G) [60]. Also, the dermal tissue was restored and integrated into the epidermis, with the maximum number of skin appendages and capillary hyperproliferation compared with the other groups, signifying that occurs complete wound healing.

To observe collagen deposition/production as one of the crucial parameters in the regulation of several phases of wound healing, Masson's trichrome staining was performed on tissue sections on day 14. As depicted in Fig. 11, the immature collagen fibers were disorderly arranged in the control group (Fig. 11A); by contrast, the free PVA/CS NFs treated wounds, albeit still not entirely normal, indicate more content of collagen and more organized collagen alignment (Fig. 11B). Whereas thyme-loaded NFs (Fig. 11C) and ginger-loaded NFs (Fig. 11D) have shown more collagen accumulation and thick wavy collagen fibers than animals treated with free

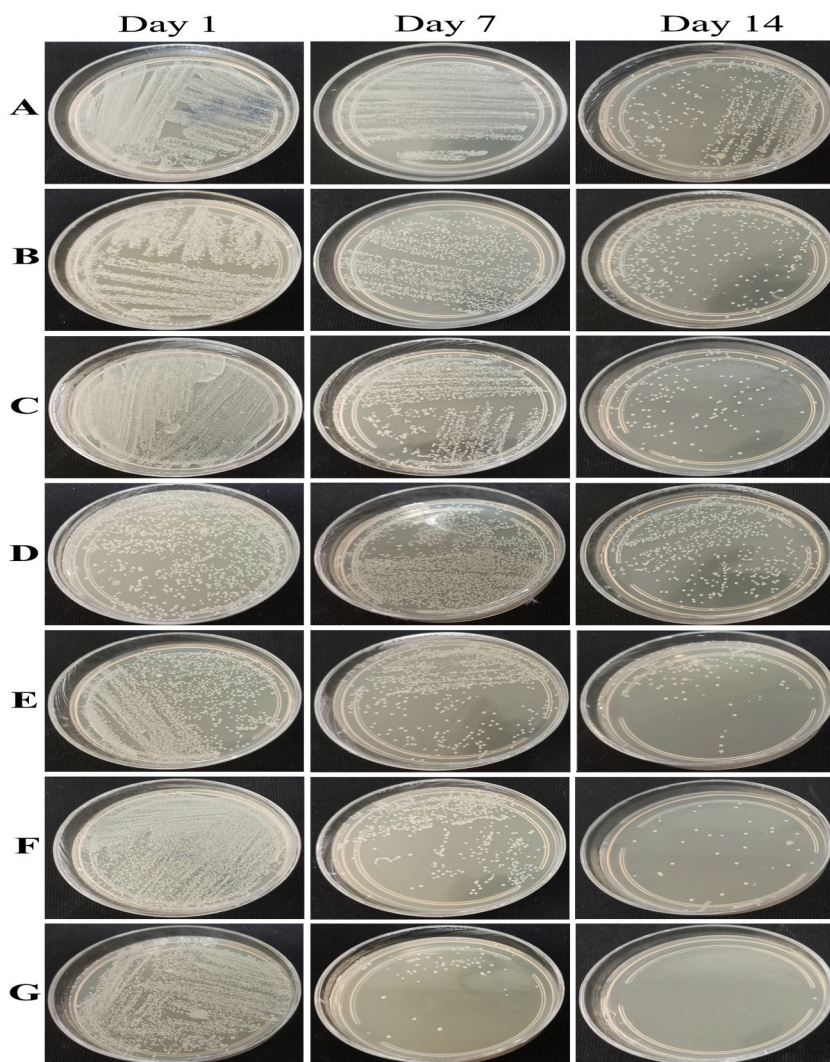


Fig. 9. Representative images of the bacterial culture from infected wounds on days 1, 7 and 14 in different treated groups: negative control (A), thyme extract (B), ginger extract (C), free PVA/CS NFs (D), thyme-loaded NFs (E), ginger-loaded NFs (F), and ginger:thyme loaded NFs (G).

PVA/CS NFs, however, ginger: thyme loaded NFs exhibited well-developed and dense, uniform collagen bundles throughout the dermis. Therefore, the collagen content was significantly higher than that of the other groups and appeared newly formed hair follicles, sweat glands, and blood vessels (Fig. 11E).

These results indicate that concurrent incorporation of thyme and ginger extract into the nanofibrous mats could not only inhibit bacteria infection but also accelerate wound healing by promoting the regeneration of skin tissue. Probably, these effects arose from the combined bioactive components presenting in both thyme and ginger extracts that explored and approved their therapeutic effects in several studies [17,29,47,56–58].

4. Conclusion

Herein, we developed a composite PVA/CS nanofibrous mat containing two efficient herbal extracts of *Thymus vulgaris* and *Zingiber officinale* intended for promoting infection-induced wound healing. The electrospun ginger:thyme-loaded NFs exhibited the nano-scale fiber diameter with appropriate morphology and loaded amounts without adverse interactions between the constituents. The obtained mats also displayed high liquid absorption capacity, high porosity, and hydrophilic surface. In addition, they showed significant antioxidant activity, as well as their release profile was continuous and sustainable. Altogether, they were able to significantly inhibit the growth of both Gram-positive and Gram-negative bacteria. *In vivo* experiments over infected wounds demonstrated that the proposed NFs provided the maximum reduction in the wound area, faster wound closure, and accelerated skin regeneration. Microbiological and histopathological studies at the wound site also approved the complete inhibition of bacterial growth, the entire regeneration of skin layers, and the formation of collagen fibers and appendages. Overall, as a natural multi-component loaded-wound

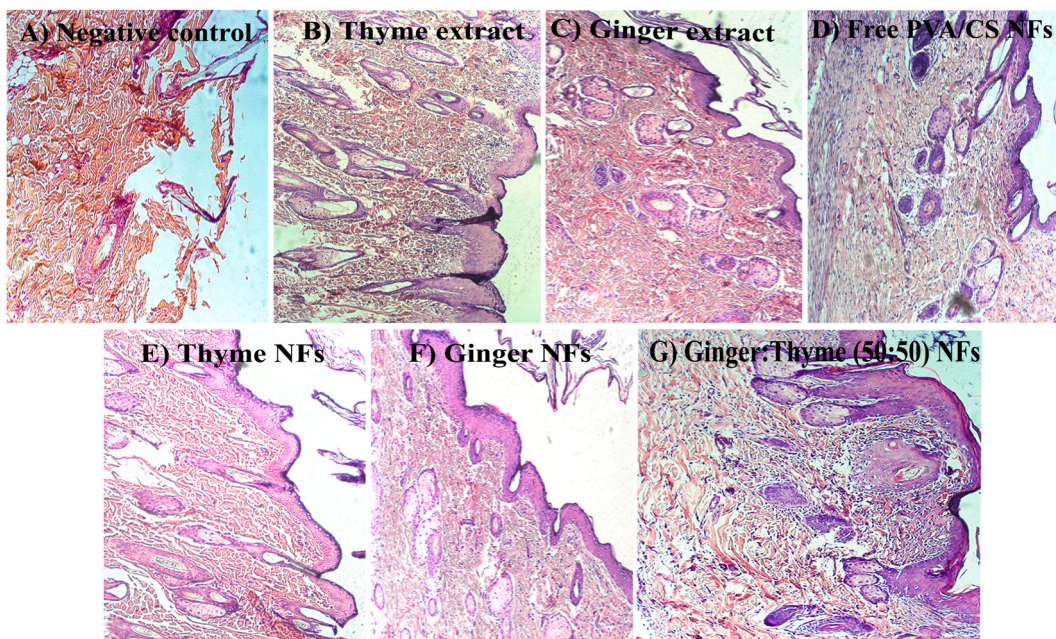


Fig. 10. H&E staining images of the wound tissue on the 14th day in different treated groups (magnification, $\times 100$); A) negative control, B) thyme extract, C) ginger extract, D) free PVA/CS NFs, E) thyme-loaded NFs, F) ginger-loaded NFs, and G) ginger:thyme loaded NFs.

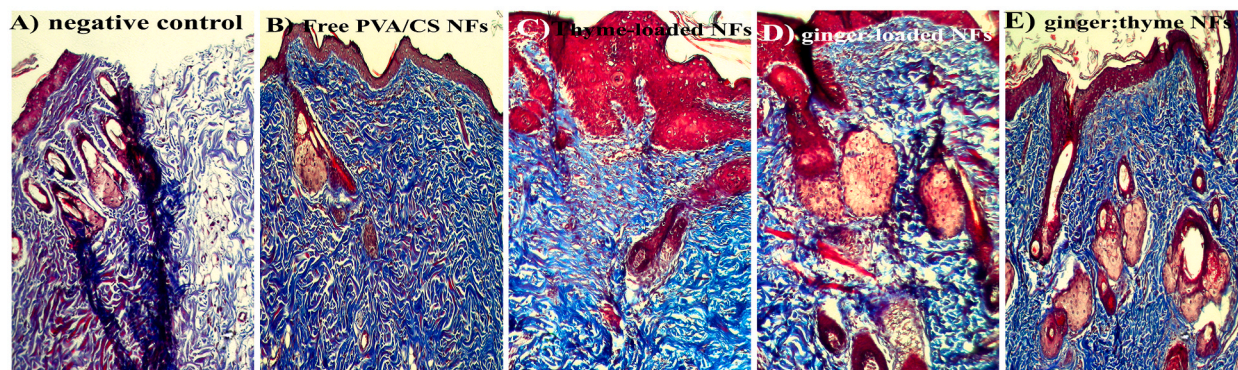


Fig. 11. Masson's trichrome staining images of wounds treated by: negative control (A), free PVA/CS NFs (B), thyme-loaded NFs (C), ginger-loaded NFs (D), and ginger:thyme loaded NFs (E). (Blue color denotes the distribution of collagen, Mag = $\times 100$). (For interpretation of the references to color in this figure legend, the reader is referred to the Web version of this article.)

dressings, ginger: thyme-loaded nanofibrous mats render a promising solution for handling wound infections and skin tissue regeneration.

Funding

This work was supported by Kermanshah University of Medical Sciences, Grant No. 4010322.

Ethics approval and consent to participate

The procedures were performed following the ethical approval of Kermanshah University of Medical Sciences (IR.KUMS.AEC.1401.005) and the animal studies were performed under the EU Directive 2010/63/EU for animal experiments and subsequent amendments or comparable ethical standards.

Consent for publication

All the authors have approved this article and agreed with the submission.

Data availability statement

Data will be made available on request.

CRedit authorship contribution statement

Hassan Maleki: Writing – review & editing, Writing – original draft, Visualization, Validation, Supervision, Resources, Funding acquisition. **Maryam Doostan:** Methodology, Investigation, Formal analysis, Conceptualization. **Kamyar Khoshnevisan:** Writing – review & editing, Writing – original draft, Visualization, Investigation, Data curation. **Hadi Baharifar:** Writing – original draft, Software, Data curation, Conceptualization. **Saeid Abbasi Maleki:** Writing – original draft, Visualization, Validation. **Mohammad Amin Fatahi:** Writing – original draft, Methodology, Investigation, Conceptualization.

Declaration of competing interest

The authors declare the following financial interests/personal relationships which may be considered as potential competing interests.

References

- [1] P.-H. Wang, B.-S. Huang, H.-C. Horng, C.-C. Yeh, Y.-J. Chen, Wound healing, *J. Chin. Med. Assoc.* 81 (2018). https://journals.lww.com/jcma/Fulltext/2018/02000/Wound_healing.3.aspx.
- [2] J. Hwang, K.L. Kiick, M.O. Sullivan, Modified hyaluronic acid-collagen matrices trigger efficient gene transfer and prohealing behavior in fibroblasts for improved wound repair, *Acta Biomater.* 150 (2022) 138–153, <https://doi.org/10.1016/j.actbio.2022.07.039>.
- [3] K. Khoshnevisan, H. Maleki, H. Samadian, M. Doostan, M.R. Khorramizadeh, Antibacterial and antioxidant assessment of cellulose acetate/polycaprolactone nanofibrous mats impregnated with propolis, *Int. J. Biol. Macromol.* 140 (2019) 1260–1268, <https://doi.org/10.1016/j.ijbiomac.2019.08.207>.
- [4] H. Maleki, K. Khoshnevisan, S.M. Sajjadi-Jazi, H. Baharifar, M. Doostan, N. Khoshnevisan, F. Shariifi, Nanofiber-based systems intended for diabetes, *J. Nanobiotechnol.* 19 (2021) 317, <https://doi.org/10.1186/s12951-021-01065-2>.
- [5] S.P. Miguel, R.S. Sequeira, A.F. Moreira, C.S.D. Cabral, A.G. Mendonça, P. Ferreira, I.J. Correia, An overview of electrospun membranes loaded with bioactive molecules for improving the wound healing process, *Eur. J. Pharm. Biopharm.* 139 (2019) 1–22, <https://doi.org/10.1016/j.ejpb.2019.03.010>.
- [6] G. Zang, M. He, Y. Liao, M. Li, M. Hong, W. Li, Electrochemical improvement in high-voltage Li-ion batteries by electrospinning a small amount of nano-Al₂O₃ in P(MVE-MA)/P(VdF-HFP)-blended gel electrolyte, *Ionics* 28 (2022) 767–777, <https://doi.org/10.1007/s11581-021-04351-z>.
- [7] X. Cai, P. Zhu, X. Lu, Y. Liu, T. Lei, D. Sun, Electrospinning of very long and highly aligned fibers, *J. Mater. Sci.* 52 (2017) 14004–14010, <https://doi.org/10.1007/s10853-017-1529-0>.
- [8] A.R. Unnithan, A.R.K. Sasikala, P. Murugesan, M. Gurusamy, D. Wu, C.H. Park, C.S. Kim, Electrospun polyurethane-dextran nanofiber mats loaded with Estradiol for post-menopausal wound dressing, *Int. J. Biol. Macromol.* 77 (2015) 1–8, <https://doi.org/10.1016/j.ijbiomac.2015.02.044>.
- [9] D. Zhang, L. Li, Y. Shan, J. Xiong, Z. Hu, Y. Zhang, J. Gao, In vivo study of silk fibroin/gelatin electrospun nanofiber dressing loaded with astragaloside IV on the effect of promoting wound healing and relieving scar, *J. Drug Deliv. Sci. Technol.* 52 (2019) 272–281, <https://doi.org/10.1016/j.jddst.2019.04.021>.
- [10] Y. Liu, S. Zhou, Y. Gao, Y. Zhai, Electrospun nanofibers as a wound dressing for treating diabetic foot ulcer, *Asian J. Pharm. Sci.* 14 (2019) 130–143, <https://doi.org/10.1016/j.ajps.2018.04.004>.
- [11] M.M. Gonçalves, K.L. Lobsinger, J. Carneiro, G.F. Picheth, C. Pires, C.K. Saul, D.F. Maluf, R. Pontarolo, Morphological study of electrospun chitosan/poly(vinyl alcohol)/glycerol nanofibres for skin care applications, *Int. J. Biol. Macromol.* 194 (2022) 172–178, <https://doi.org/10.1016/j.ijbiomac.2021.11.195>.
- [12] D. Feldman, Poly(Vinyl alcohol) recent Contributions to engineering and medicine, *J. Compos. Sci.* 4 (2020), <https://doi.org/10.3390/jcs4040175>.
- [13] R. Primavera, B.D. Kevadiya, G. Swaminathan, R.J. Wilson, A. De Pascale, P. Decuzzi, A.S. Thakor, Emerging nano- and micro-technologies used in the treatment of type-1 diabetes, *Nanomaterials* 10 (2020) 789, <https://doi.org/10.3390/nano10040789>.
- [14] A. Manzoor, A.H. Dar, V.K. Pandey, R. Shams, S. Khan, P.S. Panesar, J.F. Kennedy, U. Fayaz, S.A. Khan, Recent insights into polysaccharide-based hydrogels and their potential applications in food sector: a review, *Int. J. Biol. Macromol.* 213 (2022) 987–1006, <https://doi.org/10.1016/j.ijbiomac.2022.06.044>.
- [15] X. Lin, C.T. Tsao, M. Kyomoto, M. Zhang, Injectable natural polymer hydrogels for treatment of knee osteoarthritis, *Adv. Healthcare Mater.* 11 (2022), 2101479, <https://doi.org/10.1002/adhm.202101479>.
- [16] M. Doostan, H. Maleki, M. Doostan, K. Khoshnevisan, R. Faridi-Majidi, E. Arkan, Effective antibacterial electrospun cellulose acetate nanofibrous patches containing chitosan/erythromycin nanoparticles, *Int. J. Biol. Macromol.* 168 (2021) 464–473, <https://doi.org/10.1016/j.ijbiomac.2020.11.174>.
- [17] M.E. Abd El-Hack, M. Alagawany, H. Shaheen, D. Samak, S.I. Othman, A.A. Allam, A.E. Taha, A.F. Khafaga, M. Arif, A. Osman, A.I. El Sheikh, S.S. Elnesr, M. Sitohy, Ginger and its derivatives as promising alternatives to antibiotics in poultry feed, *Animals* 10 (2020), <https://doi.org/10.3390/ani10030452>.
- [18] H. Abiral, J. Arikas, M. Mahardika, D. Handayani, I. Aminah, N. Sandrawati, A.B. Pratama, N. Fajri, S.M. Sapuan, R.A. Ilyas, Transparent and antimicrobial cellulose film from ginger nanofiber, *Food Hydrocolloids* 98 (2020), 105266, <https://doi.org/10.1016/j.foodhyd.2019.105266>.
- [19] L. Ngampunwetchakul, S. Toonkaew, P. Supaphol, O. Suwanton, Semi-solid poly(vinyl alcohol) hydrogels containing ginger essential oil encapsulated in chitosan nanoparticles for use in wound management, *J. Polym. Res.* 26 (2019) 224, <https://doi.org/10.1007/s10965-019-1880-8>.
- [20] B.A. Khan, S. Ullah, M.K. Khan, B. Uzair, F. Menaa, V.A. Braga, Fabrication, physical characterizations, and in vitro, in vivo evaluation of ginger extract-loaded gelatin/poly(vinyl alcohol) hydrogel films against burn wound healing in animal model, *AAPS PharmSciTech* 21 (2020) 323, <https://doi.org/10.1208/s12249-020-01866-y>.
- [21] M.P. Mani, S.K. Jaganathan, A.F. Ismail, Appraisal of electrospun textile scaffold comprising polyurethane decorated with ginger nanofibers for wound healing applications, *J. Ind. Text.* 49 (2018) 648–662, <https://doi.org/10.1177/1528083718795911>.
- [22] F.M. Abdelhamed, N.F. Abdeltawab, M.T. ElRakaiby, R.N. Shamma, N.A. Moneib, Antibacterial and anti-inflammatory activities of thymus vulgaris essential oil nanoemulsion on acne vulgaris, *Microorganisms* 10 (2022), <https://doi.org/10.3390/microorganisms10091874>.
- [23] N.H. Habashy, M.M. Abu Serie, W.E. Attia, S.A.M. Abdelgaleil, Chemical characterization, antioxidant and anti-inflammatory properties of Greek Thymus vulgaris extracts and their possible synergism with Egyptian *Chlorella vulgaris*, *J. Funct. Foods* 40 (2018) 317–328, <https://doi.org/10.1016/j.jff.2017.11.022>.
- [24] S.A. Alskahawy, H.H. Baghdadi, M.A. El-Shenawy, S.A. Sabra, L.S. El-Hosseiny, Encapsulation of thymus vulgaris essential oil in caseinate/gelatin nanocomposite hydrogel: in vitro antibacterial activity and in vivo wound healing potential, *Int. J. Pharm.* 628 (2022), 122280, <https://doi.org/10.1016/j.ijpharm.2022.122280>.

- [25] G. Nieto, Biological activities of three essential oils of the Lamiaceae family, *Medicine (Baltim.)* 4 (2017), <https://doi.org/10.3390/medicines4030063>.
- [26] H. Izgis, E. Ilhan, C. Kalkandelen, E. Celen, M.M. Guncu, H. Turkoglu Sasmazel, O. Gunduz, D. Ficai, A. Ficai, G. Constantinescu, Manufacturing of zinc oxide nanoparticle (ZnO NP)-Loaded polyvinyl alcohol (PVA) nanostructured mats using ginger extract for tissue engineering applications, *Nanomaterials* 12 (2022), <https://doi.org/10.3390/nano12173040>.
- [27] D. Serbezeanu, A. Bargan, M. Homocianu, M. Aflori, C.M. Rimbu, A.A. Enache, T. Vlad-Bubulac, Electrospun polyvinyl alcohol loaded with phytotherapeutic agents for wound healing applications, *Nanomaterials* 11 (2021), <https://doi.org/10.3390/nano11123336>.
- [28] A.K. Al-Asmari, M.T. Athar, A.A. Al-Faraidy, M.S. Almuhaiza, Chemical composition of essential oil of *Thymus vulgaris* collected from Saudi Arabian market, *Asian Pac. J. Trop. Biomed.* 7 (2017) 147–150, <https://doi.org/10.1016/j.apjtb.2016.11.023>.
- [29] F. Lu, H. Cai, S. Li, W. Xie, R. Sun, The chemical signatures of water extract of zingiber officinale Rosc, *Molecules* 27 (2022), <https://doi.org/10.3390/molecules27227818>.
- [30] H. Maleki, H. Azadi, Y. Yousefpour, M. Doostan, M. Doostan, M.H. Farzaei, Encapsulation of ginger extract in nanoemulsions: preparation, characterization and in vivo evaluation in rheumatoid arthritis, *J. Pharmaceut. Sci.* (2023), <https://doi.org/10.1016/j.xphs.2023.02.003>.
- [31] O. Koohi-Hosseiniabadi, M. Moini, A. Safarpoor, A. Derakhshanfar, M. Sepehrmanesh, Effects of dietary *Thymus vulgaris* extract alone or with atorvastatin on the liver, kidney, heart, and brain histopathological features in diabetic and hyperlipidemic male rats, *Comp. Clin. Pathol.* 24 (2015) 1311–1315, <https://doi.org/10.1007/s00580-015-2070-7>.
- [32] M. Doostan, M. Doostan, P. Mohammadi, K. Khoshnevisan, H. Maleki, Wound healing promotion by flaxseed extract-loaded polyvinyl alcohol/chitosan nanofibrous scaffolds, *Int. J. Biol. Macromol.* 228 (2023) 506–516, <https://doi.org/10.1016/j.ijbiomac.2022.12.228>.
- [33] G. Ajmal, G.V. Bonde, P. Mittal, G. Khan, V.K. Pandey, B.V. Bakade, B. Mishra, Biomimetic PCL-gelatin based nanofibers loaded with ciprofloxacin hydrochloride and quercetin: a potential antibacterial and anti-oxidant dressing material for accelerated healing of a full thickness wound, *Int. J. Pharm.* 567 (2019), <https://doi.org/10.1016/j.ijpharm.2019.118480>.
- [34] R. Ahmed, M. Tariq, I. Ali, R. Asghar, P. Noorunnisa Khanam, R. Augustine, A. Hasan, Novel electrospun chitosan/polyvinyl alcohol/zinc oxide nanofibrous mats with antibacterial and antioxidant properties for diabetic wound healing, *Int. J. Biol. Macromol.* 120 (2018) 385–393, <https://doi.org/10.1016/j.ijbiomac.2018.08.057>.
- [35] H. Maleki, H. Azadi, Y. Yousefpour, M. Doostan, M. Doostan, M.H. Farzaei, Encapsulation of ginger extract in nanoemulsions: preparation, characterization and in vivo evaluation in rheumatoid arthritis, *J. Pharmaceut. Sci.* 112 (2023) 1687–1697, <https://doi.org/10.1016/j.xphs.2023.02.003>.
- [36] A. Rostami-Vartooni, M. Alizadeh, M. Bagherzadeh, Green synthesis, characterization and catalytic activity of natural bentonite-supported copper nanoparticles for the solvent-free synthesis of 1-substituted 1H-1,2,3,4-tetrazoles and reduction of 4-nitrophenol, *Beilstein J. Nanotechnol.* 6 (2015) 2300–2309, <https://doi.org/10.3762/bjnano.6.236>.
- [37] CLSI, Clinical and Laboratory Standards Institute, Performance standards for antimicrobial disk susceptibility tests. Approved standards – twelfth edition. CLSI document M02-A12, *Natl. Comm. Clin. Lab. Stand.* 2012 10 (7) (2015) 10.
- [38] E. Gámez-Herrera, S. García-Salinas, S. Salido, M. Sancho-Albero, V. Andreu, M. Pérez, L. Luján, S. Irusta, M. Arruebo, G. Mendoza, Drug-eluting wound dressings having sustained release of antimicrobial compounds, *Eur. J. Pharm. Biopharm.* 152 (2020) 327–339, <https://doi.org/10.1016/j.ejpb.2020.05.025>.
- [39] N. Zeghad, R. Merghem, Antioxidant and antibacterial activities of *Thymus vulgaris* L, *Med. Aromat. Plant Res. J.* 58 (2013) 27–35.
- [40] E. Ewaldz, B. Brettmann, Molecular interactions in electrospinning: from polymer mixtures to supramolecular assemblies, *ACS Appl. Polym. Mater.* 1 (2019) 298–308, <https://doi.org/10.1021/acsapm.8b00073>.
- [41] H. Matsumoto, A. Tanioka, Functionality in electrospun nanofibrous membranes based on fiber's size, surface area, and molecular orientation, *Membranes* 1 (2011) 249–264, <https://doi.org/10.3390/membranes1030249>.
- [42] S. Majumder, M.A. Matin, A. Sharif, M.T. Arafat, Understanding solubility, spinnability and electrospinning behaviour of cellulose acetate using different solvent systems, *Bull. Mater. Sci.* 42 (2019), <https://doi.org/10.1007/s12034-019-1857-6>.
- [43] M. Koosha, H. Mirzadeh, Electrospinning, mechanical properties, and cell behavior study of chitosan/PVA nanofibers, *J. Biomed. Mater. Res., Part A* 103 (2015) 3081–3093, <https://doi.org/10.1002/jbm.a.35443>.
- [44] Z. Cui, Z. Zheng, L. Lin, J. Si, Q. Wang, X. Peng, W. Chen, Electrospinning and crosslinking of polyvinyl alcohol/chitosan composite nanofiber for transdermal drug delivery, *Adv. Polym. Technol.* 37 (2018) 1917–1928, <https://doi.org/10.1002/adv.21850>.
- [45] S.G.G. Aziz, H. Almasi, Physical characteristics, release properties, and antioxidant and antimicrobial activities of whey protein isolate films incorporated with thyme (*Thymus vulgaris* L.) extract-loaded Nanoliposomes, *Food Bioprocess Technol.* 11 (2018) 1552–1565, <https://doi.org/10.1007/s11947-018-2121-6>.
- [46] A.C.S. Valderrama, G.C. Rojas De, Traceability of active compounds of essential oils in antimicrobial food packaging using a chemometric method by ATR-FTIR, *Am. J. Anal. Chem.* 8 (2017) 726–741, <https://doi.org/10.4236/ajac.2017.811053>.
- [47] M. Rajan, A. Prabhavathy, U. Ramesh, Natural deep eutectic solvent extraction media for zingiber officinale Roscoe: the study of chemical compositions, antioxidants and antimicrobial activities, *Nat. Prod. J.* 5 (2015) 3–13, <https://doi.org/10.2174/221031550501150414094719>.
- [48] K.P. Kumar, W. Paul, C.P. Sharma, Green synthesis of silver nanoparticles with zingiber officinale extract and study of its blood compatibility, *Bionanoscience* 2 (2012) 144–152, <https://doi.org/10.1007/s12668-012-0044-7>.
- [49] T.M.S. Udenni Gunathilake, Y.C. Ching, K.Y. Ching, C.H. Chuah, L.C. Abdullah, Biomedical and microbiological applications of bio-based porous materials: a review, *Polymers* 9 (2017), <https://doi.org/10.3390/polym9050160>.
- [50] C. Huang, X. Xu, J. Fu, D.G. Yu, Y. Liu, Recent progress in electrospun polyacrylonitrile nanofiber-based wound dressing, *Polymers* 14 (2022), <https://doi.org/10.3390/polym14163266>.
- [51] S.P. Miguel, A.F. Moreira, L.J. Correia, Chitosan based-asymmetric membranes for wound healing: a review, *Int. J. Biol. Macromol.* 127 (2019) 460–475, <https://doi.org/10.1016/j.ijbiomac.2019.01.072>.
- [52] M.C. Sanchez, S. Lancel, E. Boulanger, R. Nevriere, Targeting oxidative stress and mitochondrial dysfunction in the treatment of impaired wound healing: a systematic review, *Antioxidants* 7 (2018), <https://doi.org/10.3390/antiox7080098>.
- [53] A.M. Pisoschi, A. Pop, The role of antioxidants in the chemistry of oxidative stress: a review, *Eur. J. Med. Chem.* 97 (2015) 55–74, <https://doi.org/10.1016/j.ejmech.2015.04.040>.
- [54] J. Hou, J. Yang, X. Zheng, M. Wang, Y. Liu, D.G. Yu, A nanofiber-based drug depot with high drug loading for sustained release, *Int. J. Pharm.* 583 (2020), <https://doi.org/10.1016/j.ijpharm.2020.119397>.
- [55] S. Calamak, R. Shahbazi, I. Eroglu, M. Gultekinoglu, K. Ulubayram, An overview of nanofiber-based antibacterial drug design, *Expet Opin. Drug Discov.* 12 (2017) 391–406, <https://doi.org/10.1080/17460441.2017.1290603>.
- [56] H.S. Aljabeili, H. Barakat, H.A. Abdel-Rahman, Chemical composition, antibacterial and antioxidant activities of thyme essential oil (*thymus vulgaris*), *Food Nutr. Sci.* 9 (2018) 433–446, <https://doi.org/10.4236/fns.2018.95034>.
- [57] M. Aleem, M.I. Khan, F.A. Shakshaz, N. Akbari, D. Anwar, Botany, phytochemistry and antimicrobial activity of ginger (*Zingiber officinale*): a review, *Int. J. Herb. Med.* 8 (2020) 36–49, <https://doi.org/10.22271/flora.2020.v8.i6a.705>.
- [58] S.M. Patil, R. Ramu, P.S. Shirahatti, C. Shivamallu, R.G. Amachawadi, A systematic review on ethnopharmacology, phytochemistry and pharmacological aspects of *Thymus vulgaris* Linn, *Heliyon* 7 (2021), <https://doi.org/10.1016/j.heliyon.2021.e07054>.
- [59] H. Qiu, S. Zhu, L. Pang, J. Ma, Y. Liu, L. Du, Y. Wu, Y. Jin, ICG-loaded photodynamic chitosan/polyvinyl alcohol composite nanofibers: anti-resistant bacterial effect and improved healing of infected wounds, *Int. J. Pharm.* 588 (2020), <https://doi.org/10.1016/j.ijpharm.2020.119797>.
- [60] F. Tang, J. Li, W. Xie, Y. Mo, L. Ouyang, F. Zhao, X. Fu, X. Chen, Bioactive glass promotes the barrier functional behaviors of keratinocytes and improves the Re-epithelialization in wound healing in diabetic rats, *Bioact. Mater.* 6 (2021) 3496–3506, <https://doi.org/10.1016/j.bioactmat.2021.02.041>.